

First-Principles Study of Exciton Diffusion and Dissociation in Organic Solar Cells

Xu Zhang, Zi Li and Gang Lu

**Department of Physics & Astronomy
California State University Northridge**

Supported by NSF CHE-DMS-DMR Solar Energy Initiative

Advantages of organic solar cells

- Inexpensive to fabricate
- Solution-processed in a roll-to-roll fashion with high throughput
- Low weight & flexible; Compatible with plastic substrates
- High optical adsorption coefficients that permit the use of very thin films
- Based on earth-abundant & non-toxic materials

Problem: efficiency is too low (record: 5%); the goal is 10%

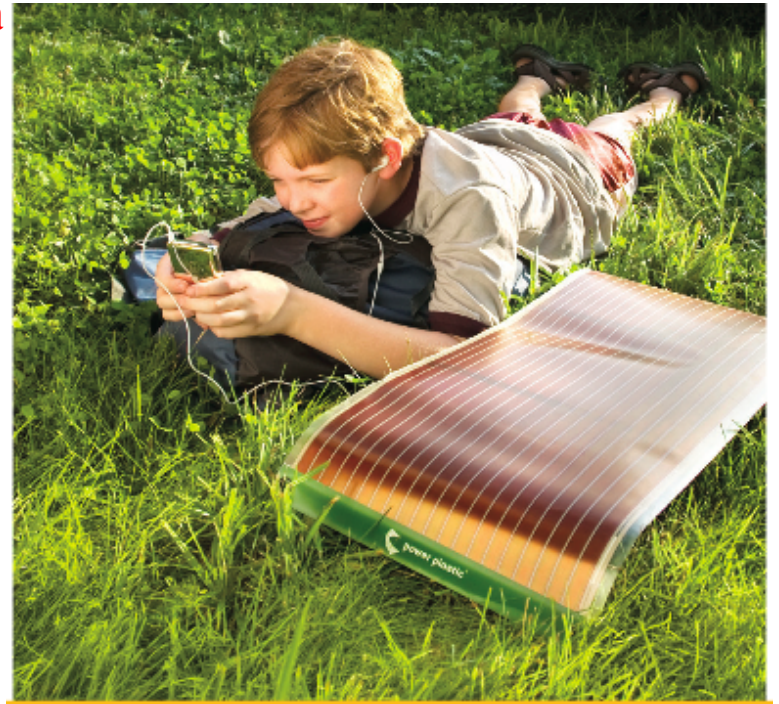
Major Bottlenecks of low efficiency

- Low exciton diffusion length
- Low carrier mobility

Plastic solar cell commercialized by Konarka



▼ Solar Powered Carport, West Palm Beach, FL

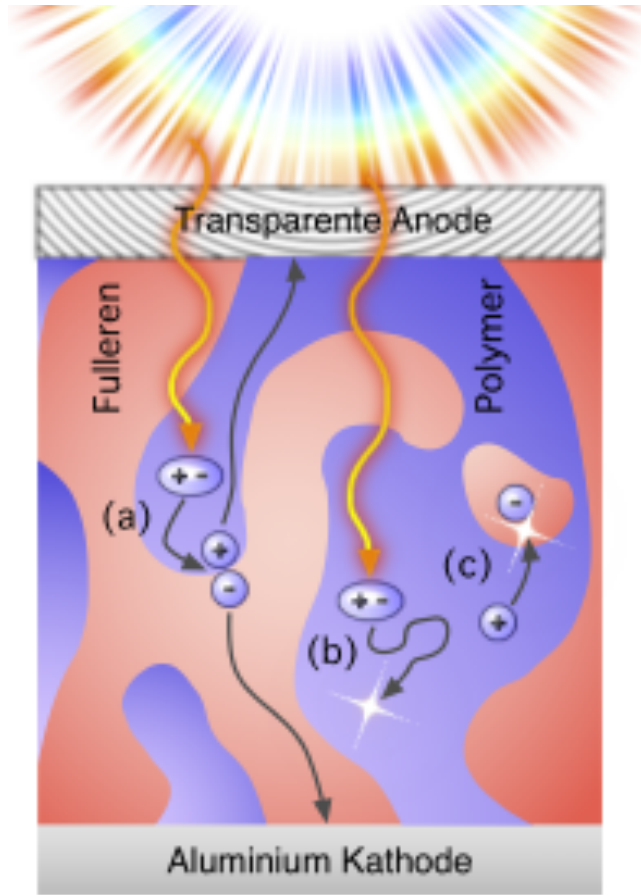


▼ Looking Through Semi-Transparent Power Plastic



Bulk Heterojunction (BHJ) Donor/Acceptor Architecture

Halls, et al., Nature (1995); Yu et al., Science (1995).

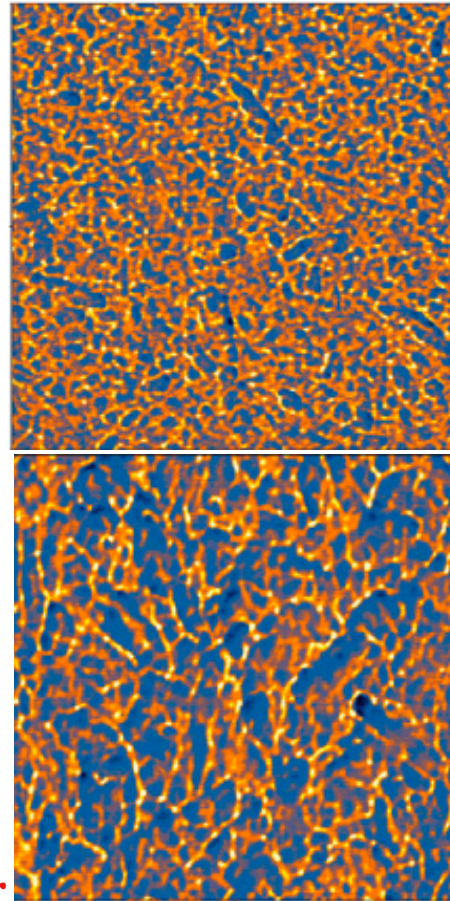


Bi-continuous donor & acceptor phases

Blue: donor (polymers)

Pink: acceptor (fullerenes)

Best material: P3HT/PCBM



2 μm x 2 μm

B. Walker (2009)

1. A photon excites donor phase creating an exciton (**Optimal band-gap to enhance adsorption**)

2. Exciton diffuses to D/A interface where it dissociates into a bound electron and hole pair. Excitons that do not reach the interface recombine and do not contribute to photocurrent (**Increase diffusion length**)

3. Bound electron-hole pair separates into free carriers (**enhance interfacial charge separation**)

4. Carrier transport to electrodes for collection (**high carrier mobility**)

First-principles prediction of carrier mobility in disordered semiconducting polymers as a function of T, carrier concentration and electric field.

Phys. Rev. B **82**, 205210 (2010)

Goal:

- (1) Develop first-principles based method to predict exciton diffusion length and exciton interfacial dissociation
- (2) Understand physical mechanisms underlying exciton dynamics
- (3) Guide/accelerate experimental discovery of more efficient materials

First-principles description of exciton dynamics

Basic Ingredients:

1. Exciton states are **localized** due to disordered nature of amorphous polymer
2. Thermal fluctuation of molecular conformations gives rise to non-adiabatic transitions between excitonic states (**phonons are important!**)

Non-adiabatic *ab initio* molecular dynamics is essential to capture these transitions

3. Linear response theory of time-dependent DFT (LR-TDDFT) for describing exciton states

At each *ab initio* MD step t :

Exciton \longleftrightarrow

$$\Psi(t) = \sum_I C_I(t) \Phi_I(t)$$

Expressed in terms of many-body

excited states Φ_I & ω_I

TDDFT
Linear
Response
theory

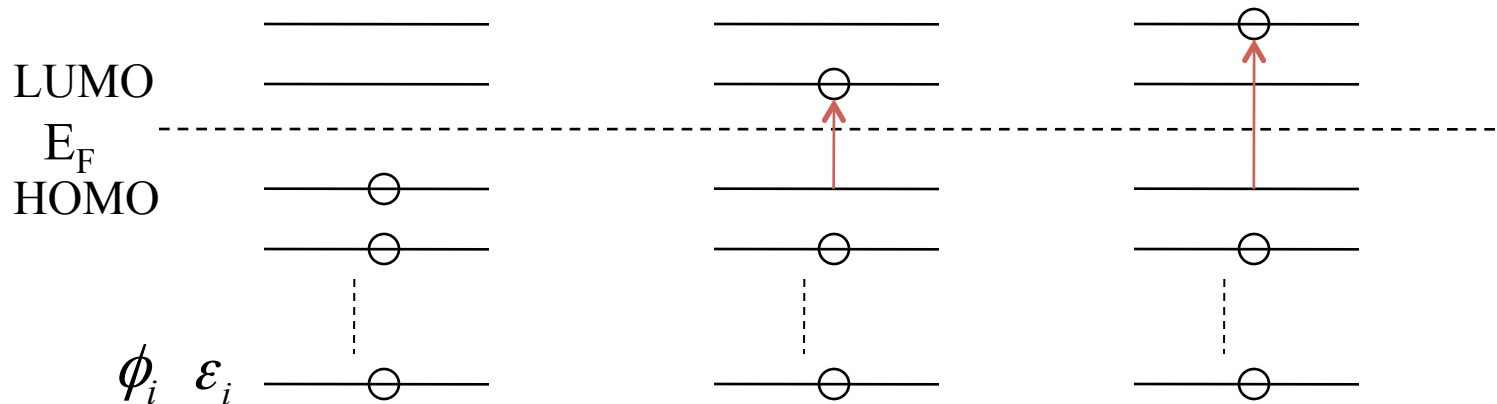
Casida's
formulation

Kohn-Sham orbital

ϕ_i & ε_i



Slater determinants (SD) for single excitations



Casida's formulation

Pseudo-eigenvalue equation based on TDDFT linear response theory:

$$\Omega F_I = \omega_I^2 F_I$$

matrix in the basis of KS states $\{ij\sigma\}$ energy of I -th excited state

$$\Omega_{ij\sigma,kl\tau} = \delta_{i,k} \delta_{j,l} \delta_{\sigma,\tau} (\varepsilon_{l\tau} - \varepsilon_{k\tau})^2 + 2\sqrt{(f_{i\sigma} - f_{j\sigma})(\varepsilon_{j\sigma} - \varepsilon_{i\sigma})}$$

$$\times K_{ij\sigma,kl\tau} \sqrt{(f_{k\tau} - f_{l\tau})(\varepsilon_{l\tau} - \varepsilon_{k\tau})}$$

occupational number energy of KS orbital

i and k run over **occupied** KS orbitals

j and l run over **unoccupied** KS orbitals

Coupling matrix describes linear response of KS effective potential to changes in charge density:

$$K_{ij\sigma,kl\tau} = \iint \phi_{i\sigma}^*(\vec{r}) \phi_{j\sigma}(\vec{r}) \frac{1}{|\vec{r} - \vec{r}'|} \phi_{k\tau}(\vec{r}') \phi_{l\tau}^*(\vec{r}') d\vec{r} d\vec{r}'$$

$$+ \iint \phi_{i\sigma}^*(\vec{r}) \phi_{j\sigma}(\vec{r}) \frac{\delta^2 E_{xc}}{\delta\rho_\sigma(\vec{r}) \delta\rho_\tau(\vec{r}')} \phi_{k\tau}(\vec{r}') \phi_{l\tau}^*(\vec{r}') d\vec{r} d\vec{r}'$$

charge density KS orbital

Assignment ansatz of Casida gives many-body wave-function of I -th excited state:

$$\Phi_I \approx \sum_{ij\sigma} \underbrace{\sqrt{\frac{\epsilon_{j\sigma} - \epsilon_{i\sigma}}{\omega_I}} F_{I,ij\sigma}}_{Z_{I,ij}} \hat{a}_{j\sigma}^+ \hat{a}_{i\sigma} \Phi_0$$

Ground state many-body wave function:
Single **Slater Determinant (SD)** of the
occupied KS orbitals

annihilation operator acting on KS orbital

$\hat{a}_{j\sigma}^+ \hat{a}_{i\sigma} \Phi_0$: one electron is excited from occupied KS state i to unoccupied KS state j
(single excitations only)

Many-body wave function of an exciton:

$$\Psi(t) = \sum_{I=0}^{\infty} C_I(t) \Phi_I(\vec{R}(t))$$

linear combination of the adiabatic ground state ($I=0$) and excited states wave functions ($I>0$); $\{\vec{R}(t)\}$: position of ions

Expectation value of single-particle operators

N-electron system, the single-particle operator: $\hat{A} = \sum_{i=1}^N \hat{a}_i$

Expectation value (**analytic result**):

$$\langle \Phi_I | \hat{A} | \Phi_I \rangle = \langle \Phi_0 | \hat{A} | \Phi_0 \rangle + \underbrace{\sum_{i,j,j'} z_{I,ij}^* z_{I,ij'} \langle \varphi_j | \hat{a} | \varphi_{j'} \rangle}_{\text{quasi-electron part}} - \underbrace{\sum_{i',j'} z_{I,i'j}^* z_{I,i'j} \langle \varphi_{i'} | \hat{a} | \varphi_{i'} \rangle}_{\text{quasi-hole part}}$$

***i*: occupied orbitals; *j*: unoccupied orbitals**

\swarrow
 expectation value in ground state

E.g., for coordinate operator:

$$\langle \Phi_I | \hat{r} | \Phi_I \rangle = \langle \Phi_0 | \hat{r} | \Phi_0 \rangle + \underbrace{\sum_{i,j,j'} z_{I,ij}^* z_{I,ij'} \langle \varphi_j | \vec{r} | \varphi_{j'} \rangle}_{\text{quasi-electron position } \vec{r}_e} - \underbrace{\sum_{i',j'} z_{I,i'j}^* z_{I,i'j} \langle \varphi_{i'} | \vec{r} | \varphi_{i'} \rangle}_{\text{quasi-hole position } \vec{r}_h}$$

\swarrow
 sum of positions of N electrons in ground state

Charge density operator:

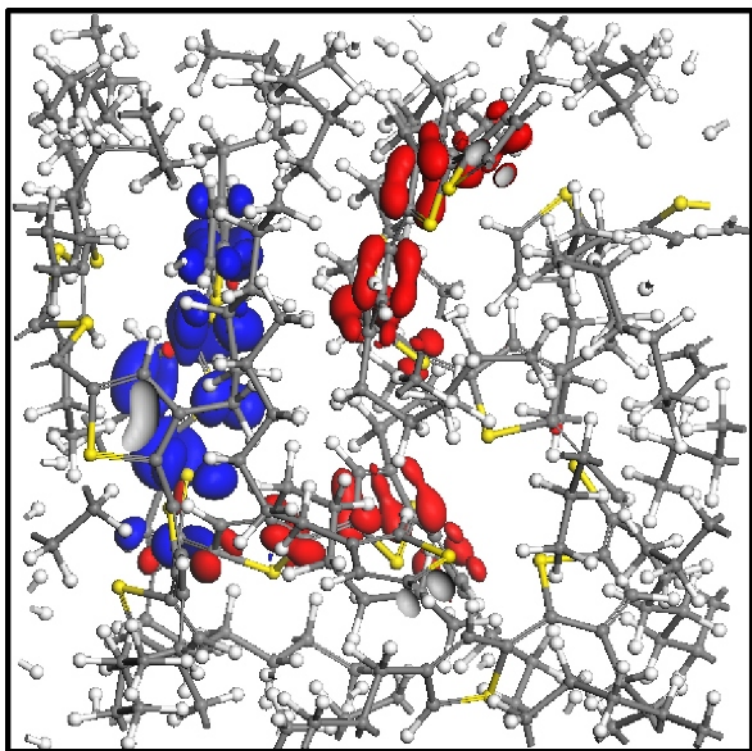
$$\hat{\rho} = \sum_{i=1}^N \delta(\vec{r} - \vec{r}_i)$$

$$\langle \Phi_I | \hat{\rho} | \Phi_I \rangle = \rho_0(\vec{r}) + \underbrace{\sum_{i,jj'} z_{I,ij}^* z_{I,ij'} \varphi_j^*(\vec{r}) \varphi_{j'}(\vec{r})}_{\text{quasi-electron charge density}} - \underbrace{\sum_{ii',j'} z_{I,ij}^* z_{I,i'j} \varphi_{i'}^*(\vec{r}) \varphi_i(\vec{r})}_{\text{quasi-hole charge density}}$$

ground state charge density

quasi-electron charge density

quasi-hole charge density



Charge density of the lowest energy exciton in disordered P3HT:

Blue: quasi-electron

Red: quasi-hole

Localized states!

18 Å

Exciton diffusion

(1) Phonon-assisted transition

(2) Spontaneous emission (decay)

(1) Phonon-assisted transition

Let exciton start in an excited many-body **pure** state I at $t=0$, i.e., $\Psi(0) = \Phi_I(\vec{R}(0))$

$t > 0$, **ions move**, the exciton state becomes a **mixed** many-body state

Introduce $C_J^{(I)}(t)$ so that $\Psi(t) = \sum_{J=0}^{\infty} C_J^{(I)}(t) \Phi_J(\vec{R}(t))$ $C_J^{(I)}(t)$: probability amplitude

$$\text{with } C_J^{(I)}(0) = \delta_{I,J}$$

Substitute $\Psi(t)$ into time-dependent many-body Schrodinger equation:

$$i\hbar \frac{\partial}{\partial t} \Psi(t) = H(\vec{R}(t)) \Psi(t)$$

↓
many-body Hamiltonian

Obtain dynamics of exciton transition:

$$\frac{\partial}{\partial t} C_J^{(I)}(t) = - \sum_K C_K^{(I)}(t) \left(\frac{i}{\hbar} \omega_K \delta_{JK} + D_{JK} \right)$$

$$D_{JK} = \left\langle \Phi_J \left| \frac{\partial}{\partial t} \right| \Phi_K \right\rangle = \sum_{i,j \neq j'} z_{I,ij}^* z_{J,ij'} d_{jj'} - \sum_{i \neq i', j} z_{I,ij}^* z_{J,i'j} d_{i'i}$$

$d_{i'i}$: non-adiabatic coupling between Kohn-Sham state i and i'

$$d_{i'i} = \left\langle \phi_{i'} \left| \frac{\partial}{\partial t} \right| \phi_i \right\rangle \approx \frac{1}{2\Delta t} (\langle \phi_{i'}(t) | \phi_i(t + \Delta t) \rangle - \langle \phi_{i'}(t + \Delta t) | \phi_i(t) \rangle)$$

Where $\phi_i(t)$ is the Kohn-Sham single particle wave function.

$|C_J^{(I)}(t)|^2$ **exciton transition probability from state I to state J at time t**

$$\gamma_{I,J}^{\text{Phonon}} = \left\langle \frac{|C_J^{(I)}(t)|^2}{t} \right\rangle_{\delta t} \text{ transition rate (average over time interval } [t, t + \delta t] \text{)}$$

Transition rates

- (2) Spontaneous emission (decay) **without phonon assistance**
Transition dipole moment approximation

$$\gamma_{I,J}^{\text{Dipole}} = \frac{4(\omega_I - \omega_J)^3 |\langle \Phi_I | \vec{r} | \Phi_J \rangle|^2}{3c^3}$$

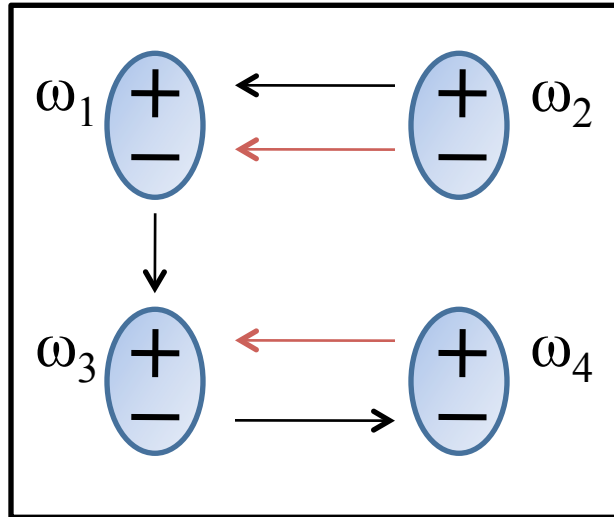
- (3) Transition rate satisfying detailed balance:

$$\gamma_{I,J} = \begin{cases} \gamma_{I,J}^{\text{Phonon}} \exp\left(-\frac{\omega_J - \omega_I}{k_B T}\right), & \text{if } \omega_J \geq \omega_I \\ \gamma_{I,J}^{\text{Phonon}} + \gamma_{I,J}^{\text{Dipole}}, & \text{if } \omega_J < \omega_I \end{cases}$$

- **Phonon assisted transition contributes to both the downhill and uphill transitions**
- **Spontaneous emission only contributes to the downhill transitions**

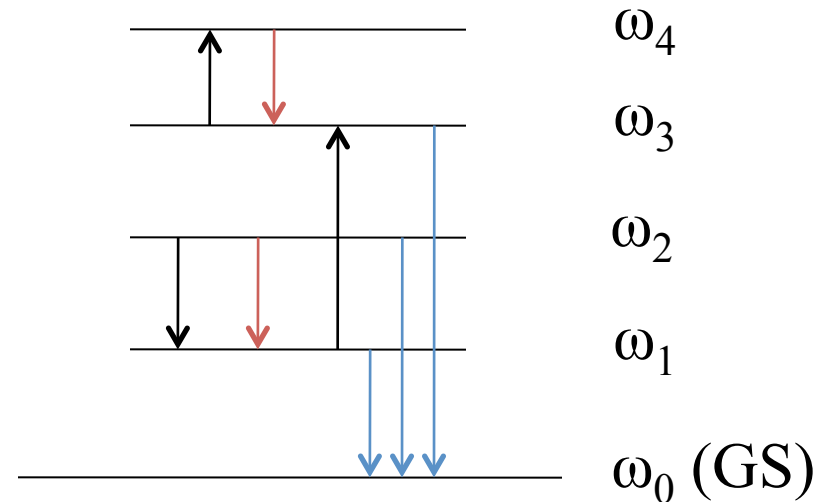
Exciton diffusion in real and energy space

Real space



$$\vec{r}_{ex} = \frac{\vec{r}_e + \vec{r}_h}{2}$$

Many-body energy space



Binding energy: 0.16 eV (disordered P3HT)
0.53 eV (single P3HT chain)

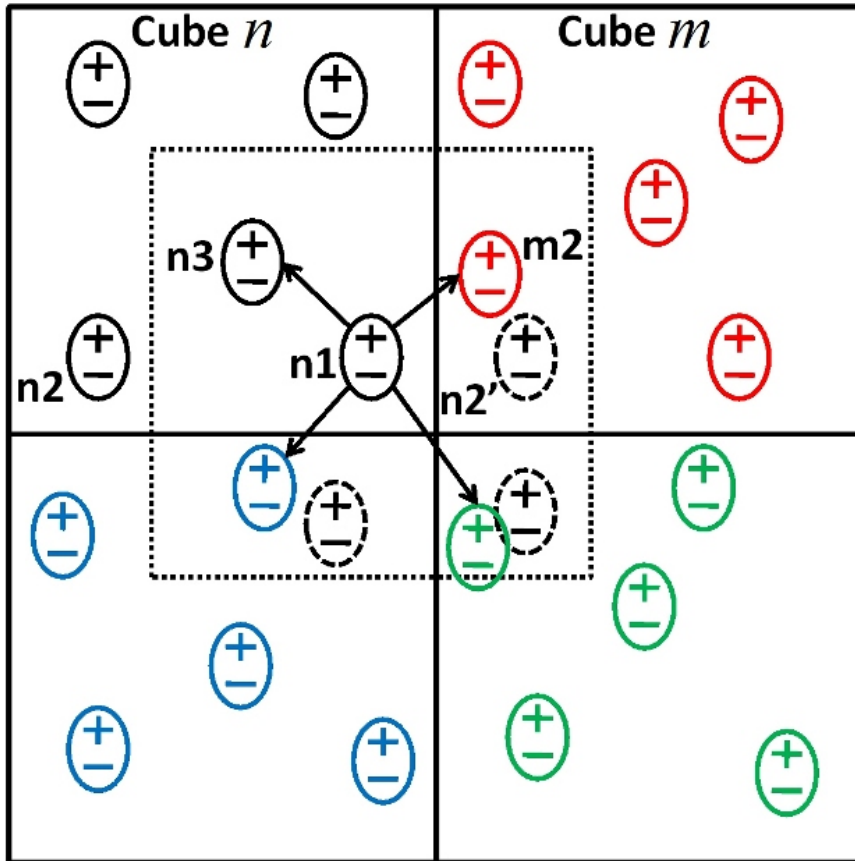
- Phonon-assisted exciton transition (rate: $10^9 \sim 10^{12} \text{ s}^{-1}$, **ps to ns**)
- Spontaneous emission (from high energy to low energy, $\leq 10^7 \text{ s}^{-1}$, **microsecond**)
- Exciton annihilation (from excited states to GS, 10^9 s^{-1} , **ps**)

Transition between exciton states Exciton diffusion in real space

Construction of macroscopic system

Two daunting challenges: (1) to model macroscopic system with microns dimensions
 (2) to model amorphous disordered system

“Macroscopic” system: $l_x \times l_y \times l_z$ cubes



1. Cube n : home box in which transition rates have been calculated (5 excitons here)
2. KS states in each cube are **randomly selected and rotated** from MD snap-shots (to model amorphous structure)
3. Determine exciton position in each box

To determine inter-cube transition rate:

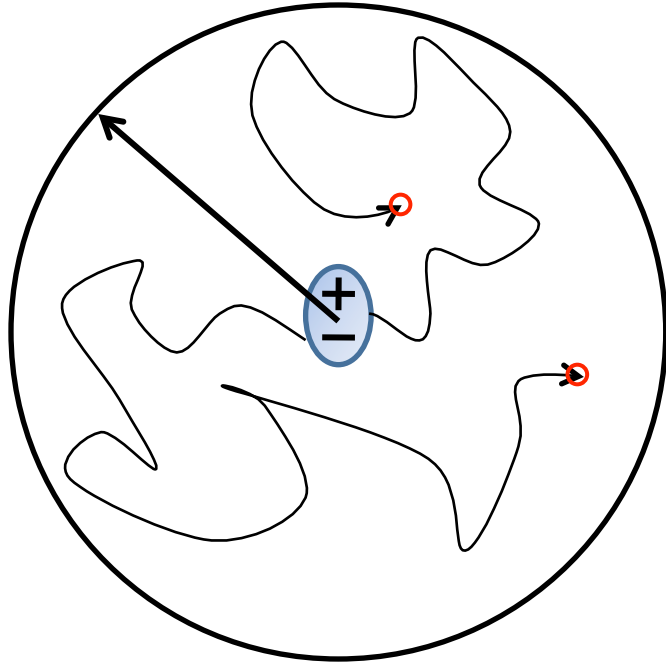
E.g. considering exciton $n1$:

Translate cube n so that $n1$ is at the center of the cube (dashed cube); etc. The transition rate $\gamma_{n1,m2}$ is replaced by $\gamma_{n1,n2'}$ or $\gamma_{n1,n2}$

$n1$ can only hop to 4 neighboring excitons

Monte Carlo Calculation

Maximum distance of exciton diffusion: **diffusion length**



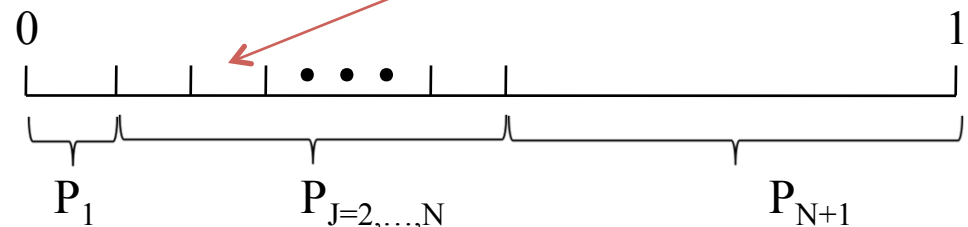
○ Annihilation site

- Step 1: select an exciton I
- Step 2: list event table with transition probability
 - Annihilation: $P_1 = \gamma_{I,0} \times \Delta t$
 - Inter-state transition: $P_{J=2,3,\dots,N} = \gamma_{I,J} \times \Delta t$
 - Stay in the same state: $P_{N+1} = 1 - (P_1 + P_2 + \dots + P_N)$

N : number of excitons in a cube (54)

Δt : time step in MC (10 fs)

- Step 3: for a given **random number**, execute an MC move



Diffusion length $L_D = \langle d_{\max} \rangle$

Diffusion time $\tau = \langle t \rangle$

Diffusivity $D = \frac{\langle d_{\max}^2 \rangle}{3 \langle t \rangle}$



- Step 4: continue Step 3 until exciton annihilates for one MC trajectory.

- Step 5: continue for many trajectories.

- Step 6: take average of all trajectories

- Step 7: continue for different excitons

Simulation Flowchart

1. Static relaxation of initial structure (636 atoms); heat up to desired temperatures; stay at the desired temperature with 500 MD steps to reach thermal equilibrium. MD step size 1 fs. Simulation performed by VASP.
2. Run a micro-canonical MD for 1000 fs. Determining ω_I & Φ_I and spontaneous emission rate at each MD step. 6 occupied KS orbitals and 9 unoccupied KS orbitals are considered to produce 54 excited states.
3. To calculate phonon-assisted transition rate $\gamma_{I,J}^{\text{phonon}}(t)$ at time t , TDDFT is run from t to $t+\delta t$ ($\delta t=100$ fs) with the KS states determined from MD.
4. Construct macroscopic system using $l_x \times l_y \times l_z$ cubes.
5. Perform Monte Carlo calculation.

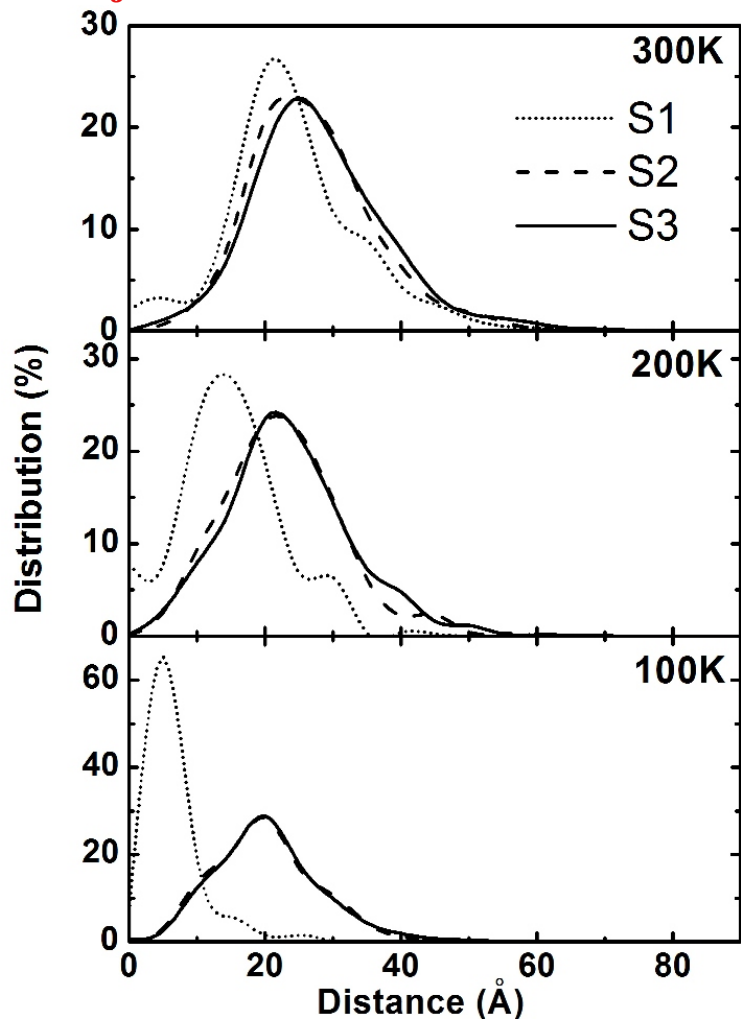
Results for disordered P3HT

Statistics (percentage) of exciton diffusion distance for 10^4 trajectories

Three exciton states are examined:

- S1: lowest energy exciton state
- S2: exciton state ~ 0.6 eV higher than S1
- S3: exciton state ~ 1.2 eV higher than S1

- Higher energy excitations diffuse farther
- S2&S3 have (almost) the identical diffusion behavior
- Diffusion length increases with temperature; particularly so for lower energy excitons



Calculated diffusion length L_D (nm), lifetime τ (ns), and diffusivity D ($10^{-9}\text{m}^2/\text{s}$)

	300K			200K			100K		
	s1	s2	s3	s1	s2	s3	s1	s2	s3
L_D	2.6	3.0	3.1	1.7	2.5	2.6	0.9	2.2	2.3
τ	2.0	1.8	1.7	3.6	3.9	3.8	4.2	4.4	4.3
D	4.1	5.3	6.0	1.0	1.9	2.0	0.2	1.3	1.4

Experimental results at 300K:

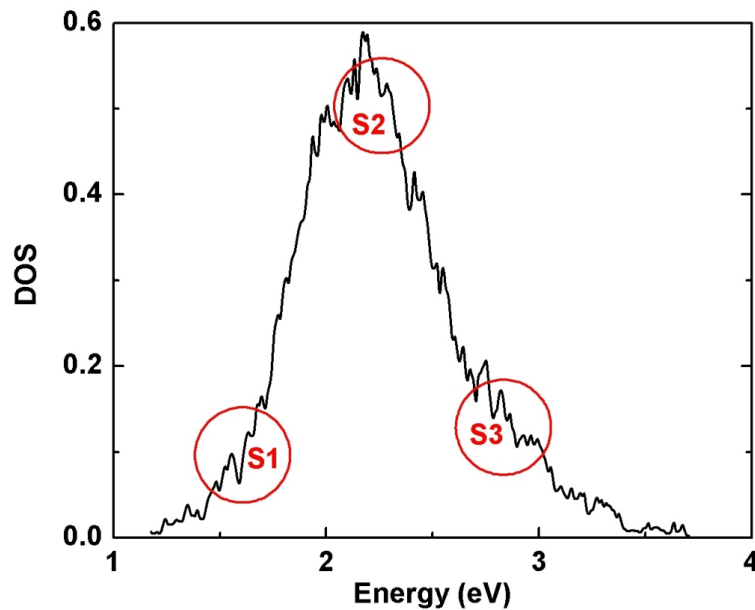
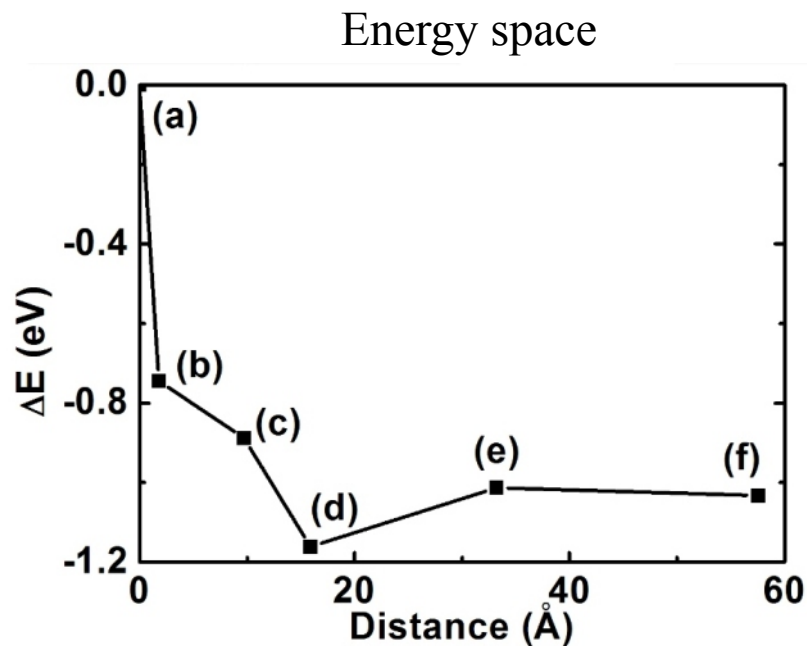
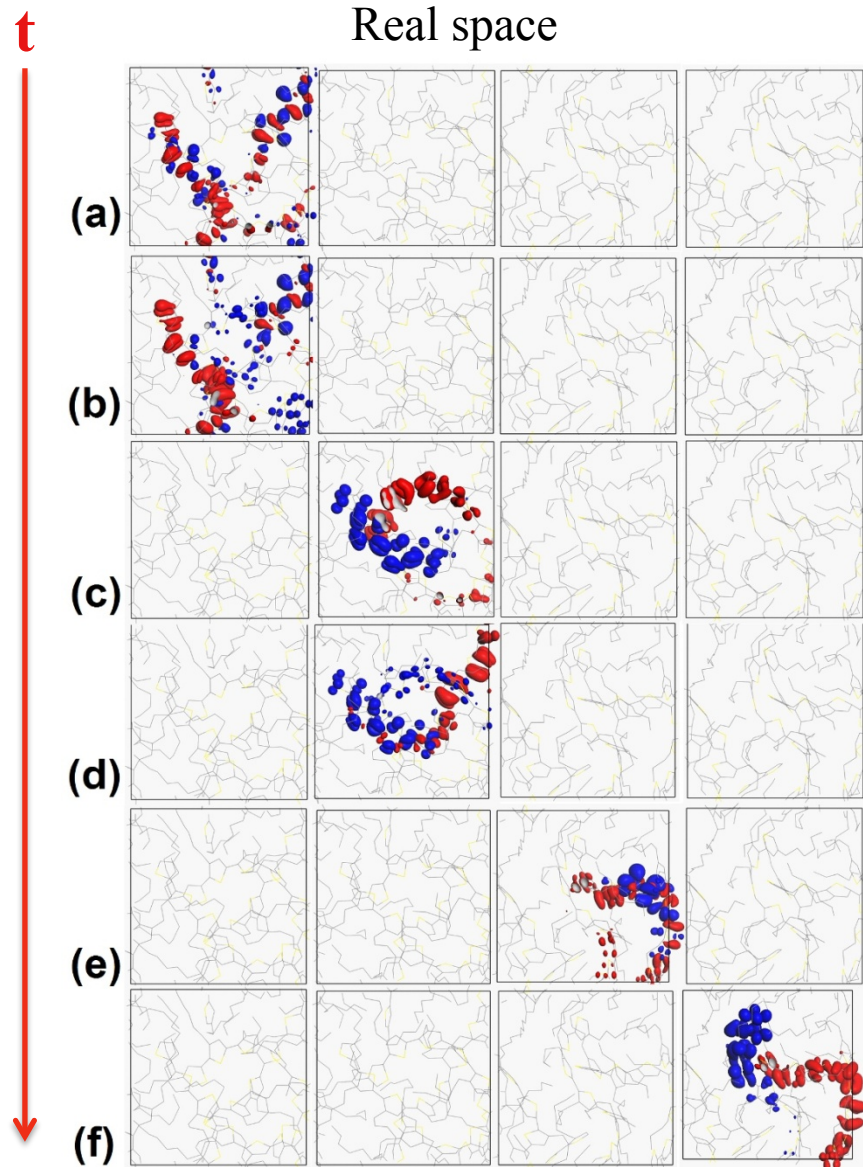
$$L_D = 4 \text{ nm} \quad [1]$$

$$L_D = 2.6 \sim 5.3 \text{ nm} \quad [2]$$

[1] L. Luer, H. J. Egelhaaf, D. Oelkrug, G. Cerullo, G. Lanzani, B. H. Huisman, D. de Leeuw, *Org. Electron.* 5, 83 (2004).

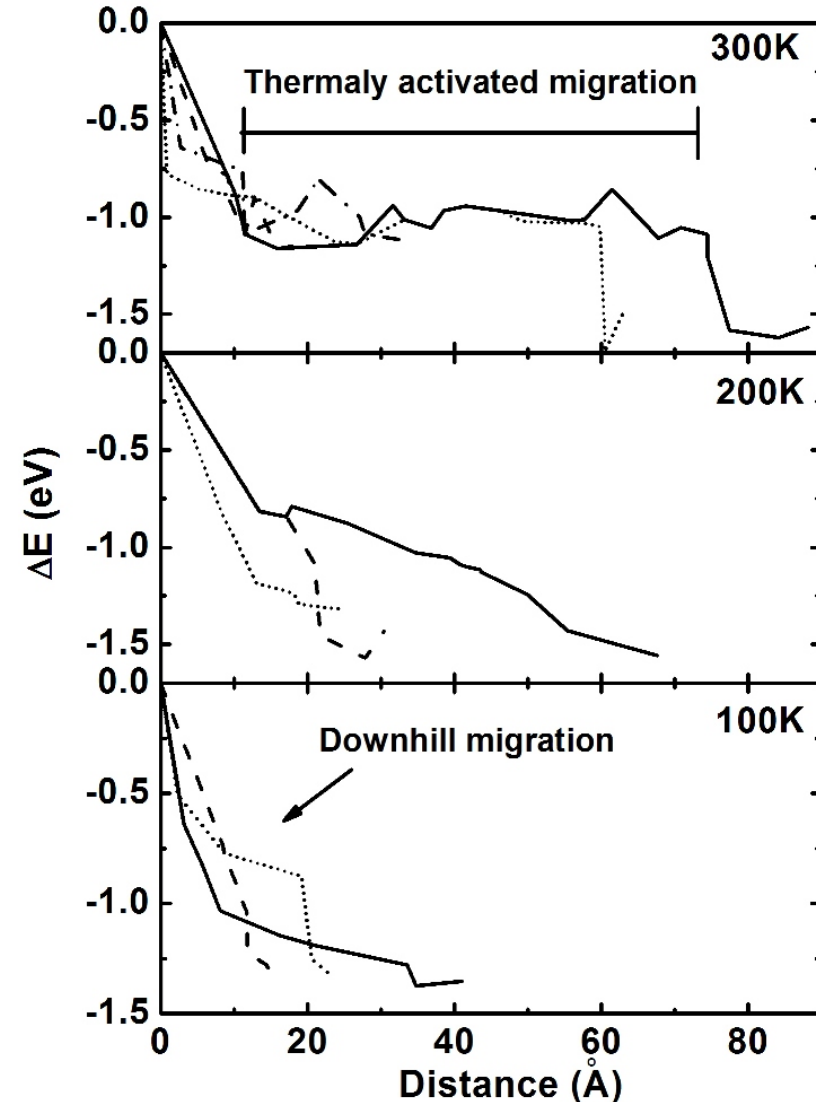
[2] J. E. Kroeze, T. J. Savenije, M. J. W. Vermeulen, and J. M. Warman, *J. Phys. Chem. B* 107, 7696 (2003).

Exciton diffusion (S3) in real and energy space at 300K



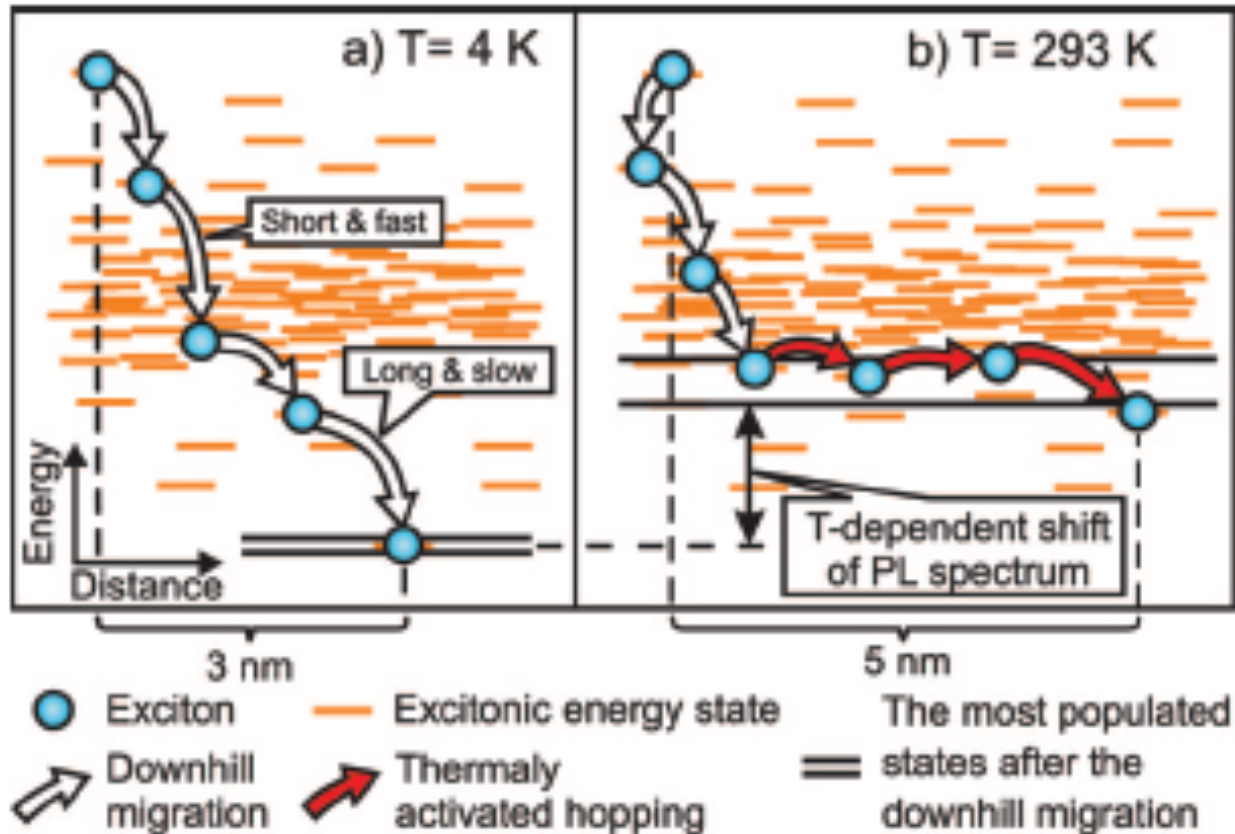
Exciton diffusion mechanisms

exciton energy vs. diffusion distance



- **Downhill migration:** quickly dumps energy, but has minor contribution to diffusion length - doesn't need phonons
- **Thermally activated migration:** dominate exciton diffusion without significant change of exciton energy - need phonon assistance
- At low temperature, downhill migration dominates
- At higher temperature, downhill migration followed by thermally activated migration

Two regimes for exciton diffusion*



(1) Downhill migration, temperature regime 4 - 150 K

(2) Thermally activated migration, temperature regime > 150 K

*O. V. Mikhnenko, F. Cordella, A. B. Sieval, J. C. Hummelen, P. W. M. Blom, and M. A. Loi, *J. Phys. Chem. B* 2008, 112, 11601–11604

Interfacial Exciton Dissociation

Simplified Fewest switch surface hopping (FSSH)

In original FSSH [1], an electron (exciton) always stays at **one** excited state at any given time, but it can hop from one state to another. Here, we use a simplified FSSH method [2], in which a hop-rejection in the original FSSH is replaced by multiplying the hop probability with Boltzmann factor for an energetic upward transition. The probability from state J to K during the time-step δt is

$$g_{JK} = \begin{cases} [\max(0, \frac{b_{KJ}\delta t}{a_{JJ}})] \cdot \exp(\frac{-(\epsilon_K - \epsilon_J)}{kT}), & \epsilon_K > \epsilon_J \\ [\max(0, \frac{b_{KJ}\delta t}{a_{JJ}})], & \epsilon_K \leq \epsilon_J \end{cases}$$

where

$$a_{KJ} = C_K^*(t)C_J(t) \quad b_{KJ} = -2\text{Re}(a_{KJ}D_{KJ})$$

With FSSH, we know precisely which state the exciton is at in any time. We can determine the position and charge density of the exciton (and quasi-electron and quasi-hole). Examine electron-hole (e-h) distance and charge distribution as a function of time

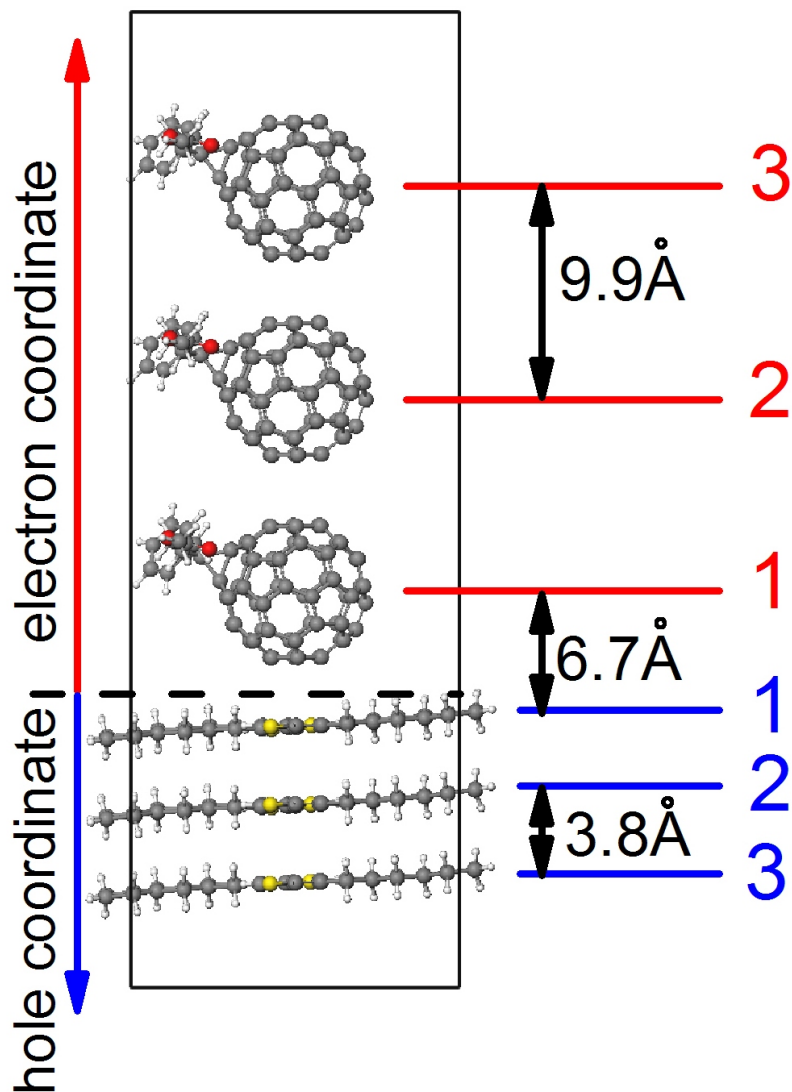
[1] J.C. Tully, J. Chem. Phys. 93 1061 (1990).

[2] W. R. Duncan, C. F. Craig, and O. V. Prezhdo, J. Am. Chem. Soc. **129**, 8528 (2007).

Simulation Flowchart

1. Static relaxation of initial structure; heating system to desired temperature; stay at the desired temperature with 500 MD steps to reach thermal equilibrium. MD step size 1 fs. The simulation performed by VASP.
2. Run a micro-canonical MD for 1000 fs. Determining ω_I & Φ_I at each MD step. 3 occupied KS orbitals and 9 unoccupied KS orbitals are used to obtain 27 excited states. The non-adiabatic coupling and position of Kohn-sham states are also determined.
3. Choose different (~ 100) initial structures from the MD trajectory, each with 200 fs long.
4. For each selected short trajectory, FSSH evolution of the exciton state is performed.
 - (1) choose the initial exciton with the shortest e-h distance
 - (2) evolve $C_J(t)$ and calculate the hopping probability
 - (3) generate different (~ 100) random number sequences to determine the exciton trajectories and the corresponding position and charge density
 - (4) average over different random number sequences.
5. Take ensemble average of the different trajectories

Exciton dissociation at P3HT/PCBM interface



Simulation box: $48.0\text{\AA} \times 16.2\text{\AA} \times 15.7\text{\AA}$

Lowest interfacial exciton state energy: 0.20 eV

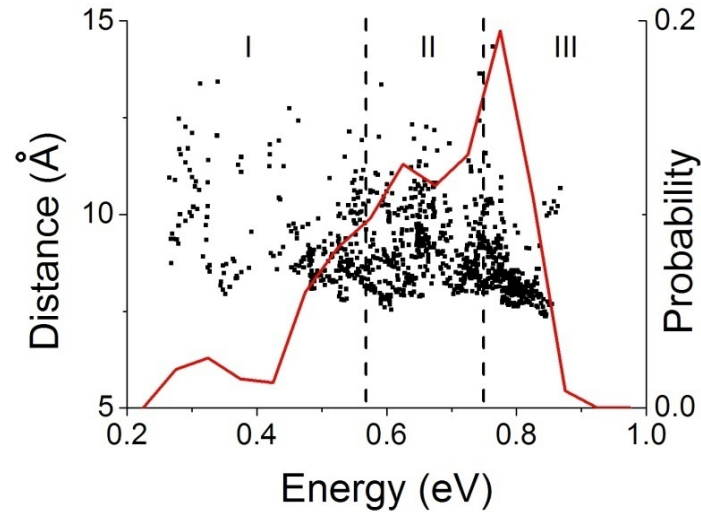
Band gap by ΔSCF : 0.55 eV

Interfacial exciton binding energy: 0.35 eV

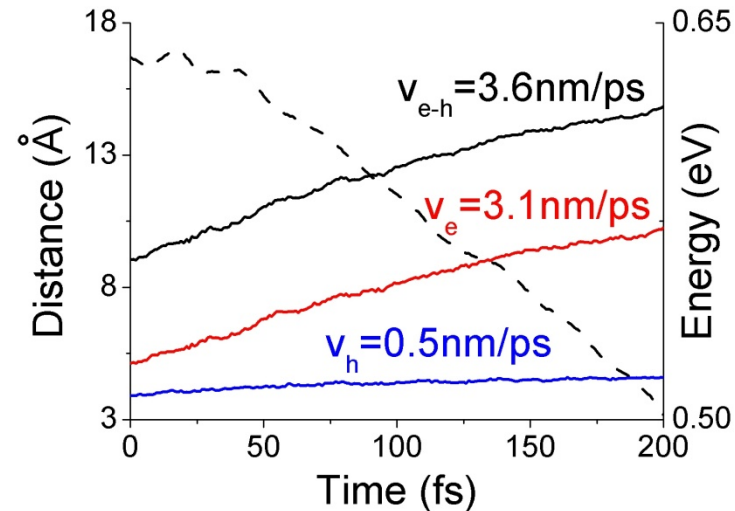
Experimental estimate of binding energy:

0.1-1 eV

Exciton dissociation process



Distribution of initial exciton states:
e-h distance: 7-11 Å
Exciton energy: 0.5-0.8 eV



Interfacial electron moves faster than hole, similar to the case in **bulk**, in which electron mobility is larger than hole.

Energy decreases from 0.64 to 0.5 eV, providing a driving force for dissociation.

e-h distance (black solid line) and exciton energy (black dash line) vs. time

Estimate of dissociation timescale

According to Onsager theory [1], Coulomb **capture radius** r_c is defined as the distance at which the Coulomb attraction energy equals the thermal energy $k_B T$.

$$r_c = \frac{e^2}{4\pi\epsilon_r\epsilon_0 k_B T}$$

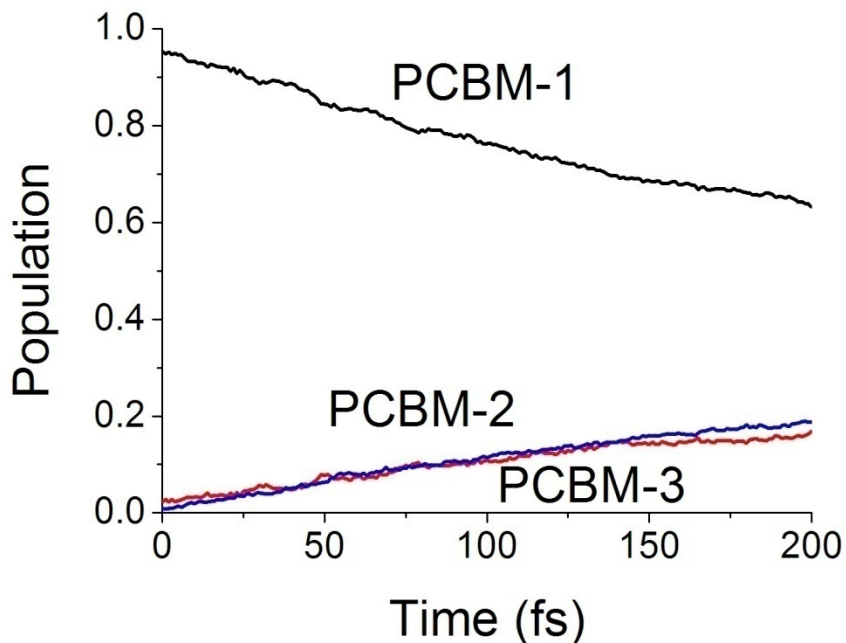
With $\epsilon_r = 4$ and $T = 300$ K, we have $r_c = 13.9$ nm

We assume that (i) once the e-h distance is larger than r_c , the dissociation process completes; (ii) the electron and hole dissociate with a constant velocity (3.1 nm/ps for e^- and 0.5 nm/ps for h^+), we can estimate dissociation time of **3.9 ps**, consistent with experimental result **4.0 ps** [2].

[1] L. Onsager, Physical Review **54**, 554 (1938).

[2] I. W. Hwang, D. Moses, and A. J. Heeger, J. Phys. Chem. C **112**, 4350 (2008).

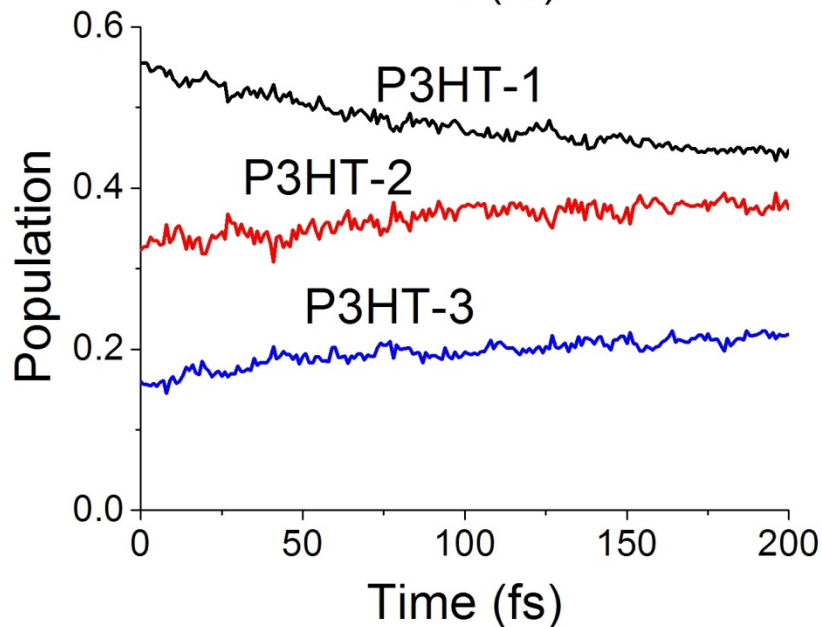
Charge separation



Quasi-electron:

At beginning, charge mainly localized on PCBM-1.

In time, the population on PCBM-1 decreases, but the population on PCBM-2 and PCBM-3 increases



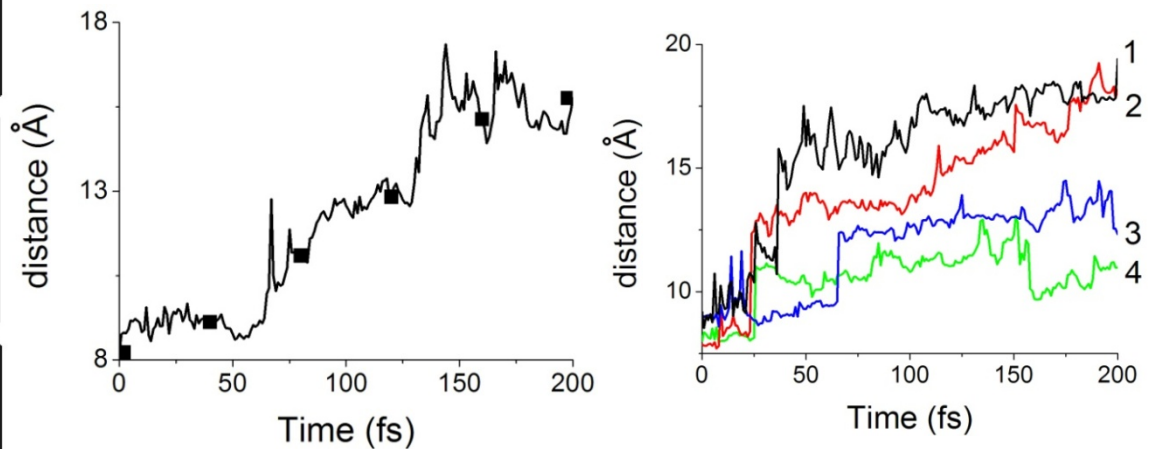
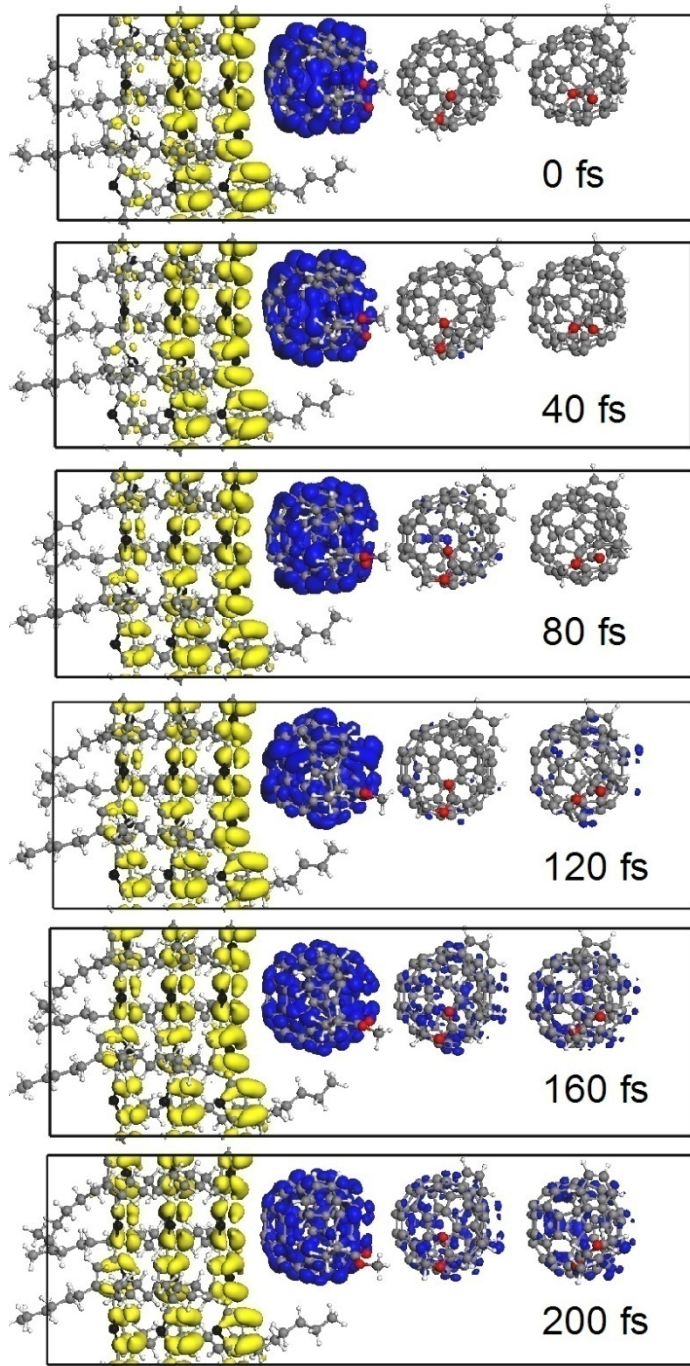
Quasi-hole:

At beginning, delocalized on all three P3HT. The farther the molecule, the smaller the population

In time, the population on P3HT-1 decreases, population on P3HT-2 and P3HT-3 increases

Clear evidence of charge separation across interface

Exciton dissociation from one MD trajectory



In this example, e-h distance increases with time

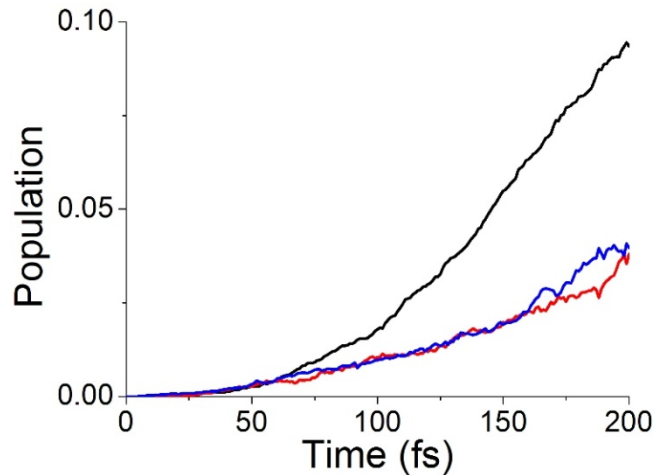
$t=0$, e^- on the PCBM-1 and h^+ delocalized on the first and second P3HT.

$t=200$ fs, significant charge separation

Exciton could have different dissociation behaviors as shown in trajectory 1-4 (**charge trapped in 4**)

Other processes at P3HT/PCBM interface

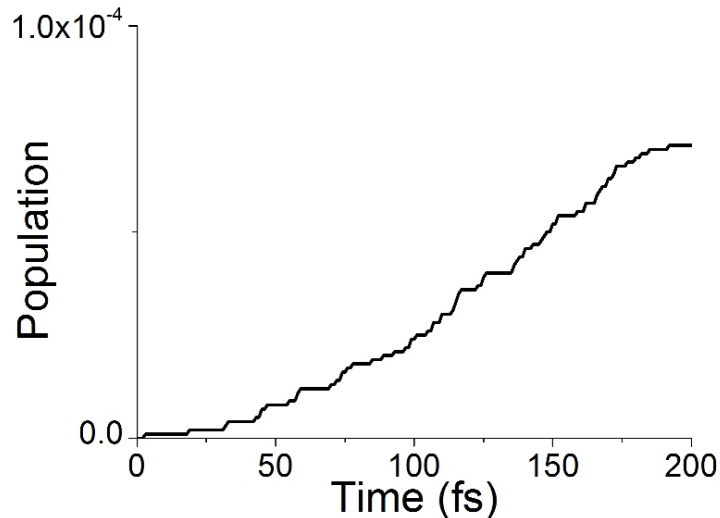
population of the lowest three states



Exciton relaxation from higher to lower excited states:

- Estimated time scale: **2.2 ps**
- Time scale similar to exciton dissociation, competition of the two processes

population of the ground state



Exciton from the lowest excited state to ground state (recombination process):

- Estimated time scale: **2.8 ns**
- Time scale much longer than dissociation, negligible influence on dissociation process